GEOLOGY | THE GEOLOGICAL SOCIETY OF AMERICA®

https://doi.org/10.1130/G46422.1

Manuscript received 21 January 2019
Revised manuscript received 29 June 2019
Manuscript accepted 1 July 2019

Published online 6 September 2019

Paleogene global cooling–induced temperature feedback on chemical weathering, as recorded in the northern Tibetan Plateau

Xiaomin Fang[1,2], Albert Galy[3], Yibo Yang[1,2], Weilin Zhang[1,2], Chengcheng Ye[2] and Chunhui Song[4]
[1]CAS Center for Excellence in Tibetan Plateau Earth Sciences, Chinese Academy of Sciences, Beijing 100101, China
[2]Key Laboratory of Continental Collision and Plateau Uplift, Institute of Tibetan Plateau Research, Chinese Academy of Sciences, Beijing 100101, China
[3]Centre de Recherches Pétrographiques et Géochimiques, UMR7358, CNRS, Université de Lorraine, 54500 Nancy, France
[4]School of Earth Sciences & Key Laboratory of Western China's Environmental Systems (MOE), Lanzhou University, Lanzhou 730000, China

ABSTRACT

Plate-tectonic processes have long been thought to be the major cause of the Cenozoic global carbon cycle, and global cooling by uplift of the Tibetan Plateau through enhancing silicate weathering and organic carbon burial and/or by weathering of obducted ophiolites during the closure of the Neo-Tethys Ocean. However, the imbalance resulting from accelerated CO_2 consumption and a relatively stable CO_2 input from volcanic degassing during the Cenozoic should have depleted atmospheric CO_2 within a few million years; therefore, a negative feedback mechanism must have stabilized the carbon cycle. Here, we present the first almost-complete Paleogene silicate weathering intensity (SWI) records from continental rocks in the northern Tibetan Plateau showing that silicate weathering in this tectonically inactive area was modulated by global temperature. These findings suggest that Paleogene global cooling was also strongly influenced by a temperature feedback mechanism, which regulated silicate weathering rates and hydrological cycles and maintained a nearly stable carbon cycle. It acted as a negative feedback by decreasing CO_2 consumption resulting from the lower SWI and the kinetic limitations in tectonically inactive areas.

INTRODUCTION

Postulation about the links between silicate weathering and the long-term global carbon cycle has led to an extended debate regarding the role of plate-tectonic processes, including closure of the Tethys Ocean and tectonic uplift of the Tibetan Plateau (TP), in the global carbonate-silicate geochemical cycle via the accelerated weathering of silicate rocks (Raymo and Ruddiman, 1992; France-Lanord and Derry, 1997; Kump et al., 2000; Galy et al., 2015; Jagoutz et al., 2016). Numerous studies have attributed the remarkable increase in Cenozoic seawater Sr, Li, and Os isotopes to the weathering of uplifted continental rocks (Edmond, 1992; Klemm et al., 2005; Misra and Froelich, 2012) or obducted ophiolites (Jagoutz et al., 2016) in the Intertropical Convergence Zone. Therefore, such enhanced weathering of the continent should have induced a rapid depletion of atmospheric CO_2, and requires negative feedbacks to have stabilized atmospheric CO_2 levels (Berner and Caldeira, 1997). Various negative feedback hypotheses have been proposed; e.g., organic carbon cycle (Raymo and Ruddiman, 1992), metamorphic decarbonation (Bickle, 1996), sulfur cycle (Torres et al., 2014), and temperature (T)-dependent weathering (Kump and Arthur, 1997) hypotheses. In the latter case, the negative feedback is thought to occur in areas under "weathering-limited regimes" characterized by silicate weathering rates that are controlled by kinetic (climatic) parameters (Kump et al., 2000; West et al., 2005), such as island basalt (Li and Elderfield, 2013; Li et al., 2016), continental arcs (Lee et al., 2015), and seafloor basalt (Coogan and Dosso, 2015), or by a weatherability-climate linkage (Kump and Arthur, 1997; Caves et al., 2016; Zhang and Planavsky, 2019). These hypotheses of T-dependent weathering, and other hypotheses, are difficult to test directly by studying the geological archives at a global scale (the marine record) because other parts of the world were subjected to weathering that was insensitive to T, described as "transport-limited regimes," where silicate weathering rates scaled directly with erosion (Kump et al., 2000; West et al., 2005).

Instead of building a global record, we used an alternative approach to document the changes in the continental silicate weathering flux. Our hypothesis is that the world beyond the uplifted TP is, on average, globally characterized by stable long-term erosion rates. In that case, the rapid carbon consumption produced by enhanced silicate weathering and faster burial of organic carbon in South and East Asia, where tectonic uplift promotes monsoon development, is nearly balanced by the tight link between a lower silicate weathering intensity (SWI) and global cooling. Thus, the issue of whether the SWI of continental rocks in non–Asian-monsoon regions is closely linked to kinetic parameters, e.g., pCO_2 and temperature, will be a crucial test of our working hypothesis.

During the Paleogene, the northern TP was a tectonically inactive area, and the Asian summer monsoon did not reach this region until the beginning of the Neogene (Fig. 1; Guo et al., 2008). The major tectonic uplift of that area occurred in the late Neogene (Tapponnier et al., 2001; Li et al., 2014). Here, we present the first record in this region showing a decrease in the SWI generally coupled with the global temperature during the Paleogene.

MATERIAL AND METHODS

Clay mineral records of SWI were retrieved from the Hongliugou (HLG) section in the

CITATION: Fang, X., et al., 2019, Paleogene global cooling–induced temperature feedback on chemical weathering, as recorded in the northern Tibetan Plateau: Geology, v. 47, p. 992–996, https://doi.org/10.1130/G46422.1

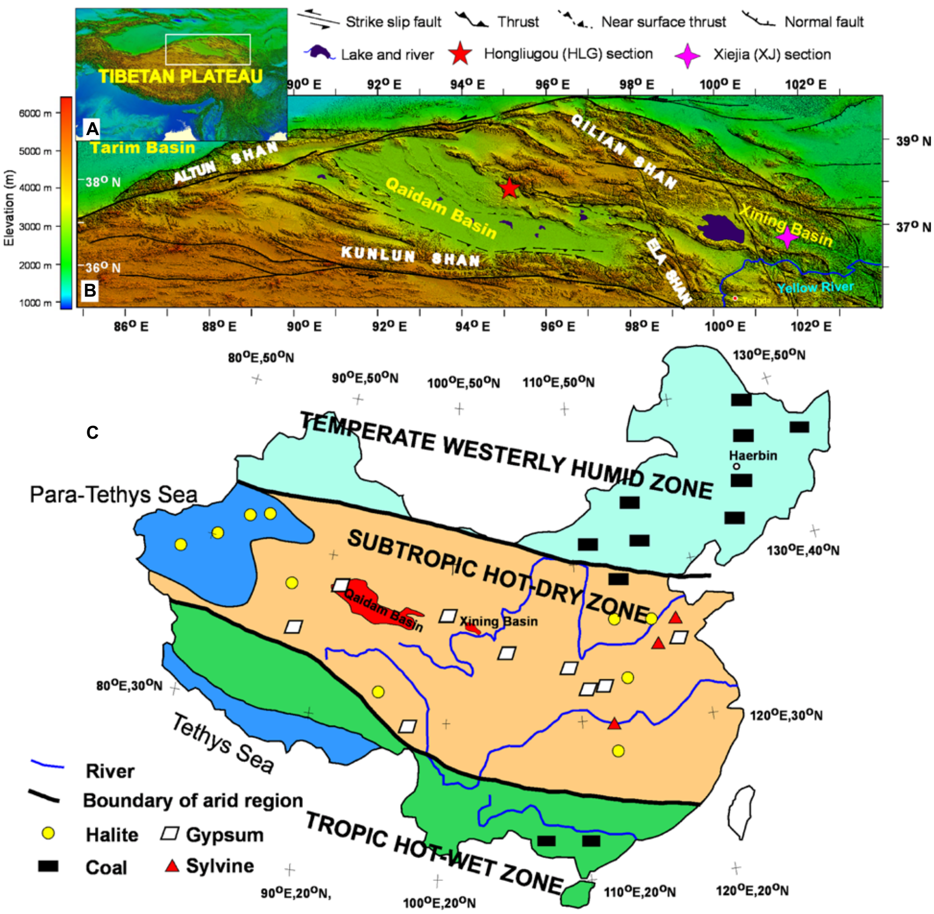

Figure 1. (A,B) Map of the northern Tibetan Plateau showing studied locations: Hongliugou (HLG) section in the Qaidam Basin, and Xiejia (XJ) section in the Xining Basin. (C) Climate zones during the Eocene of China (Guo et al., 2008).

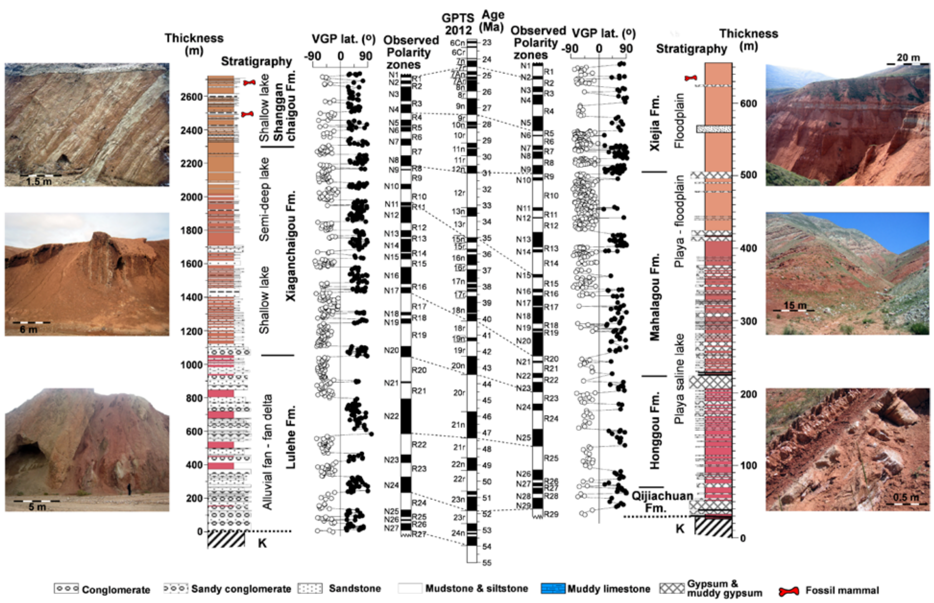

Figure 2. Lithology and magnetostratigraphy of Paleogene sediments in the Hongliugou (HLG) section in the Qaidam Basin, and the Xiejia (XJ) section in the Xining Basin, on the Tibetan Plateau. (A–D) Representative photos, lithofacies, stratigraphy, observed virtual geomagnetic pole (VGP) latitudes (lat.), and polarity zones of the HLG section (Zhang, 2007). Fm—Formation. (E) Reference geomagnetic polarity time scale (GPTS2012; Gradstein and Ogg, 2012). (F–I) Observed polarity zones and VGPs, stratigraphy, and representative photos of lithofacies of the XJ section).

Qaidam Basin and from the Xiejia (XJ) section in the Xining Basin. Both basins are large intermontane basins on the northern TP (Fig. 1). In these basins, detailed magnetostratigraphy and biostratigraphy (Dai et al., 2006; Zhang, 2007) have determined the onset of sedimentation at ca. 54–52 Ma (Fig. 2). The Paleogene strata of the HLG section are dominated in the lower part by red sandstones intercalated with thin mudstone layers representing alluvial-fan deposits, fining-upward to red-brown siltstones-mudstones embedded with green sandstones, which are interpreted as lacustrine deposits (Fig. 2; Zhang, 2007). The Paleogene strata of the XJ section are dominated by homogeneous red siltstones-mudstones intercalated with gypsum layers representing alternations of distal floodplain dry mudflat and saline lake environments (Fig. 2; Dupont-Nivet et al., 2007). The clay fractions were separated following Stokes' law and analyzed by X-ray diffraction. Aliquots of the clay-sized samples were digested with HNO_3/HF, and trace-element concentrations were measured by inductively coupled plasma–mass spectrometry. The hematite contents of bulk samples were identified by the heights of peaks at 565 nm for the first derivatives calculated from diffuse reflectance data (Deaton and Balsam, 1991).

CLAY MINERALS AS SILICATE WEATHERING PROXIES

Clay minerals in both basins are mainly composed of abundant illite/smectite mixed layers (I/S) and illite, with smectite, kaolinite, and chlorite as minor components and the occasional palygorskite (Fig. DR1 in the GSA Data Repository[1]). Clay mineral formation is linked to continental crust weathering processes characterized by the disappearance of primary silicate minerals with a loss of base ions and concomitant formation of clay minerals (Nesbitt and Young, 1982). Clay minerals in both basins are assumed to be the residual products of incongruent silicate weathering in drainage areas, and their long-term variations are weakly impacted by postdeposition diagenesis and recycled clays (see Figs. DR2–DR5 and Data Repository text). However, the protolith can have an impact on the mineralogy of clays produced by weathering. The immobile elements La and Th are more abundant in felsic rocks than in mafic rocks, and the opposite is true for Sc. Therefore, the Th/Sc ratio is a useful indicator of the provenance of felsic/mafic rock contributions (Taylor and McLennan, 1985; Cullers et al., 1988), while

[1]GSA Data Repository item 2019356, XRD data and details of the clay mineral and trace elements analyses, and test for temperature dependence of chemical weathering rate, is available online at http://www.geosociety.org/datarepository/2019/, or on request from editing@geosociety.org.

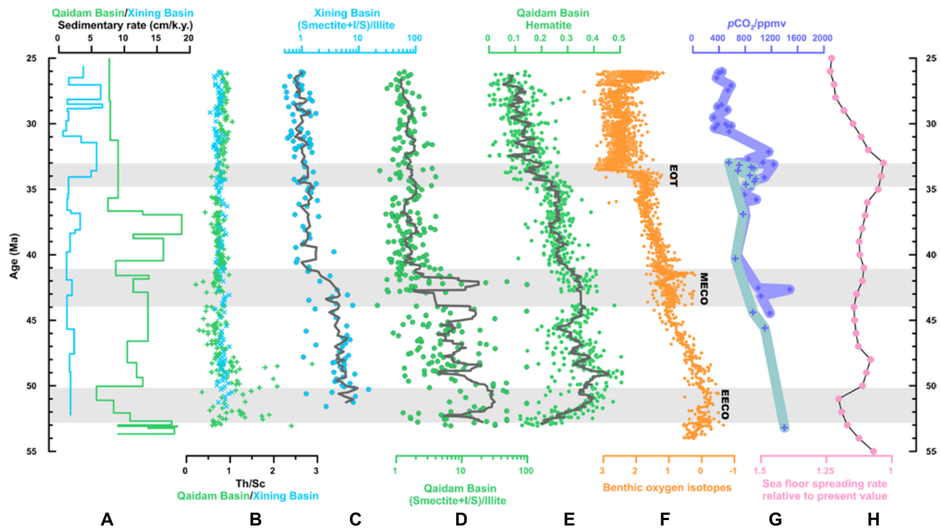

Figure 3. Mineralogy and sedimentation rate of Paleogene sediments in the Hongliugou (HLG) and Xiejia (XJ) sections in the Qaidam and Xining Basins, respectively, on the Tibetan Plateau. (A) Sedimentation rates. (B) Th/Sc ratios. (C–E) (Smectite + I/S)/illite ratios (I/S—illite/smectite mixed layers) and hematite content, with gray curve representing ~1 m.y. running averages (3-point average for C, 11-point average for D and E). Use of two different running point averages accounted for different sampling density. (F) Global marine benthic $\delta^{18}O$ record (‰, a proxy for global temperature assuming little ice volume in the Eocene; Zachos et al., 2008). EOT—Eocene-Oligocene transition; MECO—middle Eocene climatic optimum; EECO—early Eocene climate optimum. (G) Atmospheric pCO_2, where blue diamonds indicate marine phytoplanktonic $\delta^{13}C$ (Pagani et al., 2005), and blue crosses correspond to planktonic foraminiferal $\delta^{11}B$ (Pearson et al., 2009; Anagnostou et al., 2016). (H) Seafloor spreading rate (Muller et al., 2008).

La/Th should yield a relatively stable value in fine-grained sediments (McLennan et al., 1980). Felsic and mafic rocks are present in the catchments of both basins (Bureau of Geology and Mineral Resources of Qinghai Province, 1989). However, La/Th and Th/Sc in the clay fractions of both sections show very limited variability (Fig. 3; Figs. DR2 and DR3), indicating that the source rock was well mixed by riverine transport prior to deposition, and suggesting a negligible provenance control.

Overall, the clay mineralogy in both sections is likely to represent an invaluable archive to record the past catchment SWI. Chlorite and illite are predominant under cold and/or arid environments, whereas smectite, I/S, and kaolinite reflect a greater SWI under temperate-humid climates (e.g., Chamley, 1989). In both sections, the kaolinite content is generally <10% (Figs. DR2 and DR3), except in a short interval of the early Eocene in the HLG section, where the kaolinite content can reach ~20%. Such a low kaolinite content cannot be used as an index for weathering intensity. I/S is mostly a transitional product (Weaver, 1989), and since smectite, I/S, and illite make up ~80% of the clays, the (smectite + I/S)/illite ratio is the best candidate to trace the SWI at the scale of the drainage basins.

PALEOGENE SILICATE WEATHERING INTENSITY ON THE NORTHERN TIBETAN PLATEAU

The long-term decrease in the (smectite + I/S)/illite ratio in both sections (Fig. 3; Figs. DR2 and DR3) indicates a long-term weakening of the SWI since the early Eocene, although its absolute values are higher in the Qaidam Basin than in the Xining Basin. The northeastern TP was in the paleo-Asian interior and outside the area influenced by the paleo-Asian monsoon (Guo et al., 2008; Caves et al., 2015). The different absolute values between the two basins might have been caused primarily by a shorter distance from the Qaidam Basin to the westward moisture source, the Para-Tethys Sea (see Fig. 1). The long-term trend (Fig. 3) displays a close temporality between the relative changes in the (smectite + I/S)/illite ratio from both basins and early Cenozoic global cooling (Zachos et al., 2008) and pCO_2 drop (Pagani et al., 2005; Pearson et al., 2009; Anagnostou et al., 2016). This result suggests that global temperature may have been the first-order factor modulating the SWI. The remarkable decreases in the (smectite + I/S)/illite ratio at ca. 42 Ma might be a response to the ephemeral Antarctic glaciation, probably linked to the initial opening of the Drake Passage at ca. 41 Ma (Scher and Martin, 2006), and associated global cooling. The decrease in the SWI in this study can be related to the enhanced drying found in other sparse and low-resolution paleoclimatic records in the Xining Basin (Bosboom et al., 2014) and in the Qaidam Basin (Wang et al., 1999). The Eocene retreat of the Para-Tethys Sea (Sun and Jiang, 2013; Bosboom et al., 2014) may have also exerted some influence on climate by reducing the hydrological cycle in the northern TP, and thus weakening chemical weathering. However, the retreat of the Para-Tethys Sea occurred over the Eocene, not as an abrupt event at ca. 42 Ma. Thus, its influence would be both long-term and gradual. Local tectonic and differential uplifts are likely to be responsible for the increased sedimentation in the Xining Basin that occurred coeval with the lower sedimentation rate in the Qaidam Basin between 37 and 34 Ma (Fig. 3). The similar trend in the (smectite + I/S)/illite ratios of the two basins during that period further highlights the lack of correlation between the SWI and tectonic forcing in the area. The gradual decrease in the (smectite + I/S)/illite ratio in both sections ca. 35–33 Ma might have been a response to the global cooling associated with the onset of the permanent Antarctic ice sheet at the Eocene-Oligocene transition (EOT). Although the magnitude of the EOT event in our records is smaller than those of the middle Eocene climatic optimum (MECO) and early Eocene climate optimum (EECO) events (Fig. 3), its magnitude is clear in the Xining Basin in high-resolution records (Zhang and Guo, 2014).

Hematite is a type of iron oxide formed during soil weathering, and its relative content can serve as a SWI proxy (e.g., Clift et al., 2008). The hematite content in the HLG section exhibits a long-term decrease (Fig. 3; Fig. DR2) similar to the variations in the (smectite + I/S)/illite ratio. The long-term decrease in the hematite content also displays large fluctuations and provides a good match to the global temperature record, particularly post-MECO and at the Eocene-Oligocene boundary (Fig. 3). Together with temperature, precipitation is another key climate factor affecting chemical weathering (West et al., 2005; Maher and Chamberlain, 2014). High regional moisture levels likely occurred on the Para-Tethys Sea to the west of the studied regions (Fig. 1) during the Paleogene (Bosboom et al., 2014). Higher temperatures cause greater evaporation of the sea and produce higher moisture levels. Given the results of climate modeling of the area during the Paleogene (Ramstein et al., 1997), this moisture could have been transported to the studied regions by the westerlies, promoting rain and facilitating chemical weathering. Since this mechanism keeps pace with temperature, its effect has been encapsulated in the temperature-driven weathering record.

IMPLICATIONS FOR GLOBAL WEATHERING FEEDBACK

Global temperature seems to be the most likely candidate to explain the decrease in the SWI in the TP two basins. This might also be true in other parts of the world (beyond the impact of the Asian monsoon) where tectonic uplift was also weak during the Cenozoic. Considering an overall stable erosion rate in tectonically

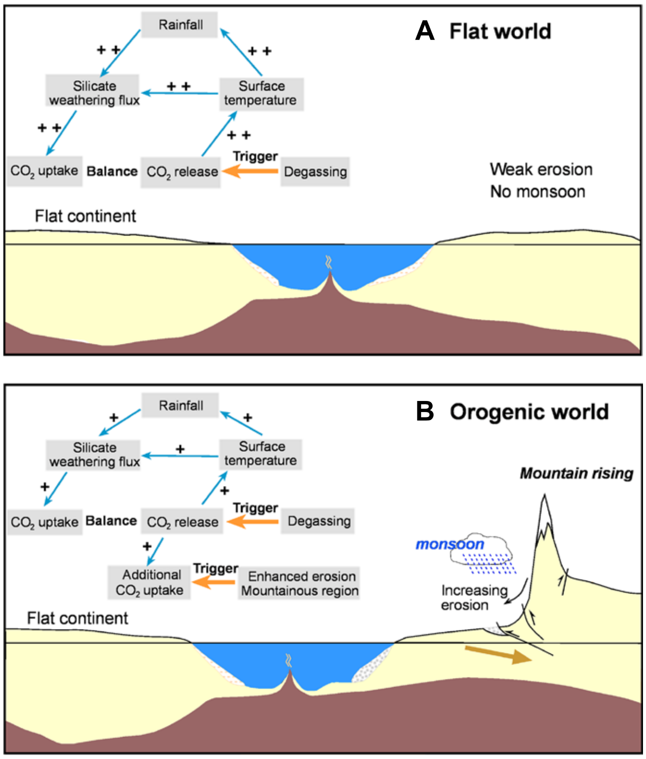

Figure 4. Conceptual models showing negative feedback mechanisms in geological carbon cycles. (A) Flat, tectonically inactive world with weak and stable erosion. (B) Orogenic world with strong erosion in orogenic belts coupled with mountain-induced strong monsoon rainfall and glacier processes. In scenario A, CO_2 degassing from Earth's mantle will be balanced by CO_2 uptake in tectonically inactive areas. Thus, any increase in degassing will lead to an increase in temperature, and ultimately will be balanced by nearly the same amount of increase in CO_2 uptake through increases in silicate weathering intensity (SWI) and thus in silicate weathering flux. In scenario B, CO_2 degassing will be quasi-balanced by combined CO_2 uptake from orogenic belts and in tectonically inactive areas. Given a constant degassing, any increase in erosion in orogenic belts will result in a decrease in SWI, possibly compensated, or even overwhelmed, by an increase in silicate weathering flux, but clearly an overall increase in CO_2 uptake in orogenic belts primarily related to enhanced organic carbon burial (France-Lanord and Derry, 1997; Galy et al., 2015). Increase in CO_2 uptake in orogenic belts will be quasi-balanced by nearly the same amount of decrease in CO_2 uptake in flat, tectonically inactive regions through decreases in temperature and, thus, in SWI and silicate weathering flux in tectonically inactive areas. Plus signs (+) mark the magnitude of carbon flux involved in various feedback processes. Large carbon flux (++) initially from degassing was involved in temperature feedbacks for scenario A, but part of this carbon flux (+) was directly consumed in orogenic belts, and the remainder (+) was involved in temperature feedbacks for scenario B.

inactive regions, the silicate weathering flux can roughly be regarded as proportional to the SWI. Thus, the correlation of SWI with global temperature (Fig. 3) suggests that global cooling could be a first-order control on the silicate weathering flux in regions beyond the impact of the Indo-Asian collision and associated development of the Asian monsoon.

Our study indeed illustrates two distinct carbon cycle patterns: one in a tectonically inactive world with less-pronounced orogenesis, giving rise to an overall stable and low global erosion flux, and the other in an orogenic world with remarkably high erosion flux derived from a combination of active orogenesis and mountain-induced heavy monsoon precipitation and glacier processes (e.g., the Himalayas; Fig. 4). In the tectonically inactive world, any imbalance in the carbon cycle from CO_2 degassing would ultimately be balanced by changes in the SWI, given an overall stable erosion flux (Fig. 4A). In contrast, in an orogenic world, any increase in erosion from the tectonically active region would lead to an overall increase in carbon sequestration (caused by extremely high erosion flux–induced increases in silicate weathering flux and organic carbon burial). However, the increase in CO_2 uptake in orogenic belts would be almost completely offset by the decrease in CO_2 uptake flux in tectonically inactive regions through decreases in global temperature and the associated lowering of the hydrological cycle. So, enhanced CO_2 consumption in tectonically active regions would be accommodated by lowered SWI across the rest of the world (Fig. 4B). Such a model is plausible since it is backed up by a first-order calculation of temperature dependence on silicate weathering rate using the Arrhenius law: $\ln(k_{post\text{-}uplift}/k_{pre\text{-}uplift}) = -Ea/R(1/T_{post\text{-}uplift} - 1/T_{pre\text{-}uplift})$, where k is silicate weathering rate; T is reaction temperature; R is a gas constant; and Ea is the activation energy; Figs. DR7 and DR8). When considering that global cooling can also induce a sluggish water cycle, the overall global cooling effect is more pronounced than that caused by the T sensitivity of silicate weathering alone (e.g., Kump et al., 2000). Because the climate system and carbon cycle evolve in a quasi–steady state, the small imbalance that results from the enhanced erosion in the tectonically active areas could drive down atmospheric pCO_2. Recent studies also have debated that other plate-tectonic processes may act as important drivers of CO_2 drawdown (Van der Meer et al., 2014; Jagoutz et al., 2016; Zhang and Planavsky, 2019). Although all of the proposed mechanisms have substantial uncertainties regarding the evolution of the Paleogene carbon cycle, our study suggests spatially variable negative feedback processes between atmospheric pCO_2 and climate, linking plate tectonics and climate.

ACKNOWLEDGMENTS

This study was co-supported by the Second Tibetan Plateau Scientific Expedition and Research (STEP) program (grant 2019QZKK0707), the Strategic Priority Research Program of the Chinese Academy of Sciences (grant XDA20070201), the National Natural Science Foundation of China (grants 41771236 and 41620104002), the External Cooperation Program (grant 131C11KYSB20160072), and the Youth Innovation Promotion Association (2018095) of the Chinese Academy of Sciences. We thank Rongsheng Yang and Xiaoming Liu for their laboratory and fieldwork assistance, as well as Lee Kump, Gaojun Li, Jeremy K. Caves Rugenstein, an anonymous reviewer, and the editor for their helpful comments.

REFERENCES CITED

Anagnostou, E., John, E.H., Edgar, K.M., Foster, G.L., Ridgwell, A., Inglis, G.N., Pancost, R.D., Lunt, D.J., and Pearson, P.N., 2016, Changing atmospheric CO_2 concentration was the primary driver of early Cenozoic climate: Nature, v. 533, p. 380–384, https://doi.org/10.1038/nature17423.

Berner, R.A., and Caldeira, K., 1997, The need for mass balance and feedback in the geochemical carbon cycle: Geology, v. 25, p. 955–956, https://doi.org/10.1130/0091-7613(1997)025<0955:TNFMBA>2.3.CO;2.

Bickle, M.J., 1996, Metamorphic decarbonation, silicate weathering and the long-term carbon cycle: Terra Nova, v. 8, p. 270–276, https://doi.org/10.1111/j.1365-3121.1996.tb00756.x.

Bosboom, R., et al., 2014, Timing, cause and impact of the late Eocene stepwise sea retreat from the Tarim Basin (west China): Palaeogeography, Palaeoclimatology, Palaeoecology, v. 403, p. 101–118, https://doi.org/10.1016/j.palaeo.2014.03.035.

Bureau of Geology and Mineral Resources of Qinghai Provence, 1991, Regional Geologic History of Qinghai Province: Beijing, Geologic Publishing House, 661 p.

Caves, J.K., Winnick, M.J., Graham, S.A., Sjostrom, D.J., Mulch, A., and Chamberlain, C.P., 2015, Role of the westerlies in Central Asia climate over the Cenozoic: Earth and Planetary Science Letters, v. 428, p. 33–43, https://doi.org/10.1016/j.epsl.2015.07.023.

Caves, J.K., Jost, A.B., Lau, K.V., and Maher, K., 2016, Cenozoic carbon cycle imbalances and a variable weathering feedback: Earth and Planetary Science Letters, v. 450, p. 152–163, https://doi.org/10.1016/j.epsl.2016.06.035.

Chamley, H., 1989, Clay Sedimentology: Berlin, Springer-Verlag, 623 p., https://doi.org/10.1007/978-3-642-85916-8.

Clift, P.D., Hodges, K.V., Heslop, D., Hannigan, R., Van Long, H., and Calves, G., 2008, Correlation of Himalayan exhumation rates and Asian monsoon intensity: Nature Geoscience, v. 1, p. 875–880, https://doi.org/10.1038/ngeo351.

Coogan, L.A., and Dosso, S.E., 2015, Alteration of ocean crust provides a strong temperature dependent feedback on the geological carbon cycle and is a primary driver of the Sr-isotopic composition of seawater: Earth and Planetary Science Letters, v. 415, p. 38–46, https://doi.org/10.1016/j.epsl.2015.01.027.

Cullers, R.L., Basu, A., and Suttner, L.J., 1988, Geochemical signature of provenance in sand-size material in soils and stream sediments near the Tobacco Root batholith, Montana, U.S.A.: Chemical Geology, v. 70, p. 335–348, https://doi.org/10.1016/0009-2541(88)90123-4.

Dai, S., Fang, X., Dupont-Nivet, G., Song, C., Gao, J., Krijgsman, W., Langereis, C.G., and Zhang, W., 2006, Magnetostratigraphy of Cenozoic sediments from the Xining Basin: Tectonic implications for the northeastern Tibetan Plateau: Journal of Geophysical Research, v. 111, B11102, https://doi.org/10.1029/2005JB004187.

Deaton, B.C., and Balsam, W.L., 1991, Visible spectroscopy—A rapid method for determining hematite and goethite concentration in geological materials: Journal of Sedimentary Research, v. 61, p. 628–632, https://doi.org/10.1306/D4267794-2B26-11D7-8648000102C1865D.

Dupont-Nivet, G., Krijgsman, W., Langereis, C.G., Abels, H.A., Dai, S., and Fang, X., 2007, Tibetan Plateau aridification linked to global cooling at the Eocene-Oligocene transition: Nature, v. 445, p. 635–638, https://doi.org/10.1038/nature05516.

Edmond, J.M., 1992, Himalayan tectonics, weathering processes, and the strontium isotope record in marine limestones: Science, v. 258, p. 1594 – 1597, https://doi/org/10.1126/science.258.5088.1594

France-Lanord, C., and Derry, L.A., 1997, Organic carbon burial forcing of the carbon cycle from Himalayan erosion: Nature, v. 390, p. 65–67, https://doi.org/10.1038/36324.

Galy, V., Peucker-Ehrenbrink, B., and Eglinton, T., 2015, Global carbon export from the terrestrial biosphere controlled by erosion: Nature, v. 521, p. 204–207, https://doi.org/10.1038/nature14400.

Gradstein, F.M., and Ogg, J.G., 2012, The chronostratigraphic scale, in Gradstein, F.M., et al., eds., The Geologic Time Scale 2012: Amsterdam, Netherlands, Elsevier, p. 31–42, https://doi.org/10.1016/B978-0-444-59425-9.00002-0.

Guo, Z.T., et al., 2008, A major reorganization of Asian climate by the early Miocene: Climate of the Past, v. 4, p. 153–174, https://doi.org/10.5194/cp-4-153-2008.

Jagoutz, O., Macdonald, F.A., and Royden, L., 2016, Low-latitude arc-continent collision as a driver for global cooling: Proceedings of the National Academy of Sciences of the United States of America, v. 113, p. 4935–4940, https://doi.org/10.1073/pnas.1523667113.

Klemm, V., Levasseur, S., Frank, M., Hein, J.R., and Halliday, A.N., 2005, Osmium isotope stratigraphy of a marine ferromanganese crust: Earth and Planetary Science Letters, v. 238, p. 42–48, https://doi.org/10.1016/j.epsl.2005.07.016.

Kump, L.R., and Arthur, M.A., 1997, Global chemical erosion during the Cenozoic: Weatherability balances the budgets, in Ruddiman, W.F., ed., Tectonic Uplift and Climate Change: Boston, Massachusetts, Springer, p. 399–426.

Kump, L.R., Brantley, S.L., and Arthur, M.A., 2000, Chemical weathering, atmospheric CO_2, and climate: Annual Review of Earth and Planetary Sciences, v. 28, p. 611–667, https://doi.org/10.1146/annurev.earth.28.1.611.

Lee, C.T.A., Thurner, S., Paterson, S., and Cao, W., 2015, The rise and fall of continental arcs: Interplays between magmatism, uplift, weathering, and climate: Earth and Planetary Science Letters, v. 425, p. 105–119, https://doi.org/10.1016/j.epsl.2015.05.045.

Li, G., and Elderfield, H., 2013, Evolution of carbon cycle over the past 100 million years: Geochimica et Cosmochimica Acta, v. 103, p. 11–25, https://doi.org/10.1016/j.gca.2012.10.014.

Li, G., et al., 2016, Temperature dependence of basalt weathering: Earth and Planetary Science Letters, v. 443, p. 59–69, https://doi.org/10.1016/j.epsl.2016.03.015.

Li, J., Fang, X., Song, C., Pan, B., Ma, Y., and Yan, M., 2014, Late Miocene–Quaternary rapid stepwise uplift of the NE Tibetan Plateau and its effects on climatic and environmental changes: Quaternary Research, v. 81, p. 400–423, https://doi.org/10.1016/j.yqres.2014.01.002.

Maher, K., and Chamberlain, C.P., 2014, Hydrologic regulation of chemical weathering and the geologic carbon cycle: Science, v. 343, p. 1502–1504, https://doi.org/10.1126/science.1250770.

McLennan, S.M., Nance, W.B., and Taylor, S.R., 1980, Rare earth element–thorium correlations in sedimentary rocks, and the composition of the continental crust: Geochimica et Cosmochimica Acta, v. 44, p. 1833–1839, https://doi.org/10.1016/0016-7037(80)90232-X.

Misra, S., and Froelich, P.N., 2012, Lithium isotope history of Cenozoic seawater: Changes in silicate weathering and reverse weathering: Science, v. 335, p. 818–823, https://doi.org/10.1126/science.1214697.

Muller, R.D., Sdrolias, M., Gaina, C., Steinberger, B., and Heine, C., 2008, Long-term sea-level fluctuations driven by ocean basin dynamics: Science, v. 319, p. 1357–1362, https://doi.org/10.1126/science.1151540.

Nesbitt, H.W., and Young, G.M., 1982, Early Proterozoic climates and plate motions inferred from major element chemistry of lutites: Nature, v. 299, p. 715–717, https://doi.org/10.1038/299715a0.

Pagani, M., Zachos, J.C., Freeman, K.H., Tipple, B., and Bohaty, S., 2005, Marked decline in atmospheric carbon dioxide concentrations during the Paleogene: Science, v. 309, p. 600–603, https://doi.org/10.1126/science.1110063.

Pearson, P.N., Foster, G.L., and Wade, B.S., 2009, Atmospheric carbon dioxide through the Eocene-Oligocene climate transition: Nature, v. 461, p. 1110–1113, https://doi.org/10.1038/nature08447.

Ramstein, G., Fluteau, F., Besse, J., and Joussaume, S., 1997, Effect of orogeny, plate motion and land-sea distribution on Eurasian climate change over the past 30 million years: Nature, v. 386, p. 788–795, https://doi.org/10.1038/386788a0.

Raymo, M.E., and Ruddiman, W.F., 1992, Tectonic forcing of late Cenozoic climate: Nature, v. 359, p. 117–122, https://doi.org/10.1038/359117a0.

Scher, H., and Martin, E., 2006, Timing and climatic consequences of the opening of Drake Passage: Science, v. 312, p. 428–430, https://doi.org/10.1126/science.1120044.

Sun, J., and Jiang, M., 2013, Eocene seawater retreat from the southwest Tarim Basin and implications for early Cenozoic tectonic evolution in the Pamir Plateau: Tectonophysics, v. 588, p. 27–38, https://doi.org/10.1016/j.tecto.2012.11.031.

Tapponnier, P., Xu, Z.Q., Roger, F., Meyer, B., Arnaud, N., Wittlinger, G., and Yang, J.S., 2001, Oblique stepwise rise and growth of the Tibet Plateau: Science, v. 294, p. 1671–1677, https://doi.org/10.1126/science.105978.

Taylor, S.R., and McLennan, S.M., 1985, The Continental Crust: Its Composition and Evolution: Oxford, UK, Blackwell Scientific, 312 p.

Torres, M.A., West, A.J., and Li, G., 2014, Sulphide oxidation and carbonate dissolution as a source of CO_2 over geological timescales: Nature, v. 507, p. 346–349, https://doi.org/10.1038/nature13030.

Van Der Meer, D.G., Zeebe, R.E., van Hinsbergen, D.J., Sluijs, A., Spakman, W., and Torsvik, T.H., 2014, Plate tectonic controls on atmospheric CO_2 levels since the Triassic: Proceedings of the National Academy of Sciences of the United States of America, v. 111, p. 4380–4385, https://doi.org/10.1073/pnas.1315657111.

Wang, J., Wang, Y.J., Liu, Z.C., Li, J.Q., and Xi, P., 1999, Cenozoic environmental evolution of the Qaidam Basin and its implications for the uplift of the Tibetan Plateau and the drying of Central Asia: Palaeogeography, Palaeoclimatology, Palaeoecology, v. 152, p. 37–47, https://doi.org/10.1016/S0031-0182(99)00038-3.

Weaver, C.E., 1989, Clays, Muds, and Shales: Amsterdam, Netherlands, Elsevier, Developments in Sedimentology 44, 819 p.

West, A.J., Galy, A., and Bickle, M., 2005, Tectonic and climatic controls on silicate weathering: Earth and Planetary Science Letters, v. 235, p. 211–228, https://doi.org/10.1016/j.epsl.2005.03.020.

Zachos, J.C., Dickens, G.R., and Zeebe, R.E., 2008, An early Cenozoic perspective on greenhouse warming and carbon-cycle dynamics: Nature, v. 451, p. 279–283, https://doi.org/10.1038/nature06588.

Zhang, C., and Guo, Z., 2014, Clay mineral changes across the Eocene-Oligocene transition in the sedimentary sequence at Xining occurred prior to global cooling: Palaeogeography, Palaeoclimatology, Palaeoecology, v. 411, p. 18–29, https://doi.org/10.1016/j.palaeo.2014.06.031.

Zhang, S., and Planavsky, N.J., 2019, The silicate weathering feedback in the context of ophiolite emplacement: Insights from an inverse model of global weathering proxies: American Journal of Science, v. 319, p. 75–104, https://doi.org/10.2475/02.2019.01.

Zhang, W.L., 2007, Cenozoic Uplift of the Tibetan Plateau: Evidence from High Resolution Magnetostratigraphy of the Qaidam Basin [Ph.D. thesis]: Lanzhou, China, Lanzhou University, 158 p.

Printed in USA